Heliyon 10 (2024) e31209

Contents lists available at ScienceDirect

Heliyon

journal homepage: www.cell.com/heliyon

Research article

Synergistic inhibition of ureolytic activity and growth of *Klebsiella pneumoniae in vitro* suggests cobinding of fluoride and acetohydroxamic acid at the urease active site and provides a novel strategy to combat ureolytic bacteria

Simon Svane [a], Mie C. Lyngsie [b,1], Janne K. Klitgaard [b,c], Henrik Karring [a,*]

[a] *Department of Green Technology, University of Southern Denmark, Campusvej 55, 5230, Odense M, Denmark*
[b] *Department of Biochemistry and Molecular Biology, Research Unit of Molecular Microbiology, University of Southern Denmark, Campusvej 55, 5230, Odense M, Denmark*
[c] *Institute of Clinical Research, Research Unit of Clinical Microbiology, University of Southern Denmark, J. B. Winsløws Vej 21, 2. sal, 5000, Odense C, Denmark*

ARTICLE INFO

Keywords:
Klebsiella pneumoniae
Ureolytic
Urease inhibition
Acetohydroxamic acid
Fluoride
Tannic acid
Urinary tract infection

ABSTRACT

The ability of ureolytic bacteria to break down stable urea to alkaline ammonia leads to several environmental and health challenges. Ureolytic bacteria such as *Helicobacter pylori, Klebsiella pneumoniae,* and *Proteus mirabilis* can become pathogenic and cause persistent infections that can be difficult to treat. Inhibiting urease activity can reduce the growth and pathogenicity of ureolytic bacteria. In the present *in vitro* study, we investigated the synergistic effects of tannic acid (TA) and the urease inhibitors fluoride (F^-) and acetohydroxamic acid (AHA). The concentration of AHA needed for efficient inhibition of the ureolytic activity of *K. pneumoniae* can be significantly reduced if AHA is coapplied with tannic acid and sodium fluoride (NaF). Thus, only 1.20 μmol l^{-1} AHA in combination with 0.30 mmol l^{-1} tannic acid and 0.60 mmol l^{-1} NaF delayed the onset of ureolytic pH increase by 95.8 % and increased the growth lag phase by 124.3 % relative to untreated *K. pneumoniae*. At these concentrations, without AHA, TA and NaF increased the onset of the ureolytic pH change by only 37.0 % and the growth lag phase by 52.5 %. The strong inhibition obtained with low concentrations of AHA in triple-compound treatments suggests cobinding of F^- and AHA at the urease active site and could reduce the side effects of AHA when it is employed as a drug against e.g. urinary tract infections (UTIs) and blocked catheters. This study reports the basis for a promising novel therapeutic strategy to combat infections caused by ureolytic bacteria and the formation of urinary tract stones and crystalline biofilms on catheters.

1. Introduction

Urease is a dinickel enzyme found in bacteria, fungi, algae, plants, and invertebrates [1]. The enzyme catalyses the hydrolysis of

Abbreviations: AHA, acetohydroxamic acid; JBU, jack bean urease; MIC, minimal inhibitory concentration; NaF, sodium fluoride; TA, tannic acid; TAN, total ammoniacal nitrogen; UTI, urinary tract infection.

* Corresponding author.
E-mail address: hka@igt.sdu.dk (H. Karring).
[1] Current address: The Danish Environmental Protection Agency, Tolderlundsvej 5, DK-5000 Odense C, Denmark.

https://doi.org/10.1016/j.heliyon.2024.e31209
Received 13 February 2024; Received in revised form 18 April 2024; Accepted 13 May 2024
Available online 14 May 2024

urea to ammonia (NH_3) and carbon dioxide (CO_2) and plays key roles in different infectious diseases and in ammonia emissions from agriculture [2]. Urease is a bacterial virulence factor, and the catalysed formation of NH_3 from urea is important for bacterial pathogenesis, with several ureolytic bacteria added to the WHO's list of pathogenic bacteria exhibiting broad antibiotic resistance [3]. When pathogenic ureolytic bacteria form NH_3, the pH of the surrounding tissue or medium increases, which facilitates the growth of the bacteria. *Helicobacter pylori*, which is thought to infect 50 % of the global population, employs ureolytic NH_3 production to survive in the low-pH environment of the stomach. Infection with *H. pylori* is often lifelong and has been linked to stomach ulcers and cancer. A high local concentration of NH_3 has direct cytotoxic effects on the epithelial cells lining the stomach [4,5]. It has recently been suggested that *H. pylori* may even colonize the oral cavity, making eradication difficult [6]. Several ureolytic bacteria, such as *Klebsiella pneumoniae, Proteus mirabilis,* and *Staphylococcus saprophyticus,* cause urinary tract infections, which lead to the formation of kidney and bladder stones of struvite ($MgNH_4PO_4$) and apatite ($Ca_{10}(PO_4)_6CO_3$) [4,5,7,8]. Recently, it has been shown that *K. pneumoniae* was more abundant in patients suffering from autoimmune inflammatory bowel diseases such as Crohn's disease and ulcerative colitis than in healthy controls [9], and it is suggested that *K. pneumoniae* infection may lead to an exacerbation of inflammation. Furthermore, periodontitis can lead to an expansion of *Klebsiella* species in the oral cavity, from which they can migrate to the lower digestive tract, causing the development of colitis and exacerbating existing gut inflammation [10].

Catheter-related urinary tract infections caused by ureolytic bacteria present a specific challenge for patients who experience bladder spasms as well as leakage and blockage of the catheter [11]. The long-term use of indwelling catheters (for more than 30 days) leads to near-certain colonization by microorganisms [11], while catheter blockage is observed in 40–50 % of patients [12,13]. Catheter-related urinary tract infections are initiated when *P. mirabilis* colonizes the bladder and catheter through the expression of mannose-resistant Proteus-like (MR/P) pili. Through ureolytic NH_3 production, the urine pH increases, leading to the precipitation of struvite ($MgNH_4PO_4$) and carbonate apatite ($Ca_{10}(PO_4)_6CO_3$). These inorganic crystalline deposits are then integrated into polysaccharide structures, forming a crystalline biofilm on the catheter. Biofilms protect the bacterial community from the host immune response and antibiotic treatment, making eradication very difficult. Eventually, the buildup of crystalline biofilms leads to blockage of the catheter and associated symptoms [14].

The only clinically available urease inhibitor drug for treating struvite stones and urinary tract infections caused by ureolytic bacteria is acetohydroxamic acid (AHA), which is produced under the US tradename Lithostat. AHA is a known urease inhibitor, but it also has an inhibitory effect on the growth of struvite crystals, which appears unrelated to its anti-ureolytic activity [15]. However, Lithostat is not widely used due to potential side effects such as anorexia, depression, anxiety (>10 %) and blood clots (>1 %), as well as potential teratogenesis [8,15–17]. *H. pylori* infections have traditionally been treated with a combination of antibiotics and proton pump inhibitors, but due to increasing antibiotic resistance, new therapeutic strategies, including anti-ureolytic bismuth salts, are being investigated [5]. Likewise, there is currently a need for new strategies to treat recurrent urinary tract infections and catheter blockages caused by ureolytic bacteria.

Recently, we reported that dual-compound treatment with tannic acid (TA) and sodium fluoride (NaF) significantly reduces the urease activity of *K. pneumoniae in vitro* and mitigates the emissions of NH_3 from pig manure [18,19]; in addition, dual-compound treatment with TA and AHA as well as mixtures of TA, NaF, and AHA cause synergistic inhibition of ureolytic activity in pure *K. pneumoniae* cultures and pig manure [20].

In the present work, we performed a comprehensive investigation of the synergistic effects of TA, NaF, and AHA on the ureolytic activity and growth of *K. pneumoniae in vitro* and explored how TA and NaF can be used to reduce the amount of AHA needed to inhibit ureolytic bacteria. This type of triple-compound combination provides a potential novel therapeutic strategy to fight infections caused by ureolytic bacteria, including recurring UTIs related to the use of indwelling catheters.

2. Materials and methods

2.1. Chemicals

Boric acid (10 g l^{-1} with indicator), hydrochloric acid (0.1 mol l^{-1} Reag. Ph. Eur.), and low-nitrogen sodium hydroxide (32 %) were purchased from VWR Denmark. All other chemicals were purchased from Merck and used as received. All media was autoclaved before use and stock solutions of inhibitors, phenol red etc. were sterile filtered before addition to the media.

2.2. Ureolytic bacterium and urease enzyme

The ureolytic bacterial strain *Klebsiella pneumoniae* subsp. *pneumoniae* (ATCC, 13882; DSM No., 30102) was purchased from the Leibniz Institute DSMZ-German Collection of Microorganisms and Cell Cultures and was stored in 15 % glycerol at −80 °C. Purified jack bean (*Canavalia ensiformis*) urease (JBU) (15,000–50,000 units/g) was purchased from Sigma–Aldrich and dissolved in an aqueous 15 mM KH_2PO_4 solution at pH 6.8 to give a final urease concentration of 1.0 mg ml^{-1}, corresponding to approximately 15–50 U/ml. The urease stock was stored at −20 °C.

2.3. Bacterial urease activity assay for determination of the minimal inhibitory concentrations (MICs) and anti-ureolytic effects of the test compounds

Determinations of the MICs and anti-ureolytic effects of the compounds against *K. pneumoniae* were carried out in M9-based urea medium (M9U) as described previously [19,21]. Briefly, 80 μl of M9U containing 33.9 μmol l^{-1} phenol red was added to the wells of a

96-well microtiter plate, and 20 μl aliquots of appropriate concentrations of TA, NaF, and AHA prepared in M9U medium were added after sterile filtration to yield 2-fold dilution series. For MIC value determination TA, NaF, and AHA were tested in concentration ranges 0–205 mmol l^{-1}, 0–2.46 mol l^{-1}, and 0–2.46 mol l^{-1}, respectively. In the single- and dual-compound treatments TA concentrations were in the range 0–0.4 mmol l^{-1}, NaF concentrations in the range 0–1.2 mmol l^{-1}, and AHA concentrations in the range 0–0.6 mmol l^{-1}. In the triple combination experiment with TA, NaF, and AHA, the concentration of TA was held constant at 0.3 mmol l^{-1} with NaF concentrations in the range 0–0.6 mmol l^{-1} and AHA concentrations in the range 0–10 μmol l^{-1}. The cell density of the *K. pneumoniae* overnight culture was measured as the optical density at 630 nm (OD630), after which the cells were diluted in M9U to an OD630 of 0.001. Diluted *K. pneumoniae* culture solution (100 μl, OD630 of 0.001) was then added to each well to a final volume of 200 μl per well. The MIC (OD630) for each well was measured after 20 h of incubation at 37 °C with constant aeration. In the bacterial urease activity assays, the absorbances at 557 nm and 630 nm were recorded every 15 min for 24 h at 37 °C with constant aeration in a plate reader (Synergy H1 hybrid multimode reader; Biotek). A negative growth control containing 200 μl of M9U without *K. pneumoniae*, an untreated growth control containing 100 μl of M9U and 100 μl of *K. pneumoniae* culture (with no TA, AHA or NaF), and the three respective monotherapies (with TA, AHA, or NaF) were included in all the experiments. Triplicate data (Replica 1, Replica 2, and Replica 3) for bacterial urease activity and growth collected from independent measurements on three different days were used for data analysis. An increase in the OD630 reflects bacterial growth, while the difference between the absorbances at 557 nm and 630 nm relates to the change in ureolytic pH (A557–A630) [21]. The effects of TA, NaF, and AHA or combinations of the compounds were compared primarily by the onset of the increase in the ureolytic pH, the end of the lag phase, and the rates of pH increase and bacterial growth. Due to the slow growth of urease-inhibited cells, most cultures had not reached the stationary phase at the end of the experiments (24 h). Therefore, the rates of pH increase and bacterial growth could not be calculated as described previously [19] but were instead calculated as the logarithmic linear rate. The effect of 0.3 mmol l^{-1} AHA on the ureolytic activity of *K. pneumoniae* was assessed similarly to that of the other agents, except that the plate reader used was a Varioskan LUX (Thermo Scientific, USA).

2.4. Determination of total ammoniacal nitrogen (TAN) production in K. pneumoniae cultures

K. pneumoniae cultures (200 ml) were grown overnight in M9U at 37 °C in baffled flasks with shaking at 200 rpm. Subsequently, the cultures were centrifuged, and the resulting cell pellets were resuspended in fresh M9U to a final OD630 of 0.1. Half of each resuspended cell culture was used as a negative control, while the other half was supplemented with TA, NaF, or AHA at final concentrations of 0.30 mmol l^{-1}, 0.60 mmol l^{-1}, or 10.0 μmol l^{-1}, respectively. Urea was added to both cultures to a final concentration of 2.4 g l^{-1}. The cultures were incubated at 25 °C for 5 h with shaking before the pH and OD630 were recorded. Triplicates of 10 ml samples of the control and inhibited cultures were analysed by the Kjeldahl method to determine the concentration of TAN (NH_3+NH_4^+) using a Kjeltec 8400 instrument (FOSS, Denmark). The samples were made alkaline by adding 16 ml of 32 % low-nitrogen NaOH, after which the instrument heated the sample to boiling using steam. All ammonium and ammonia present in the samples were converted to volatile ammonia by the high pH and evaporated into a titration vessel where they were automatically titrated with 0.1 mol l^{-1} HCl and then back-titrated with 10 % boric acid to determine the TAN concentration.

2.5. Enzymatic urease activity assays

Enzymatic urease activity assays using pure JBU were performed in 96-well microtiter plates as previously described [19]. In each well, 10 μl of 1.0 mg ml^{-1} JBU in 15 mmol l^{-1} KH_2PO_4 (pH 6.8) was added to 160 μl of M9U before 20 μl aliquots of appropriately diluted M9U solutions of inhibitors (AHA, NaF, or combinations of AHA and NaF) were added. Finally, 10 μl of 0.80 mol l^{-1} urea was added to each well, and the microtiter plate was incubated in a Varioskan LUX plate reader for 24 h at 37 °C. An uninhibited control sample of JBU was included in the experiment. The ureolytic activity was measured as A557, and the inhibition was quantified by the change in the initial rate of pH increase and the final pH (final A557) [19].

2.6. Data analysis

Data treatment, linear regressions, and statistical analyses were conducted in Excel and OriginPro 9.

Table 1
Mean MIC values for TA, NaF, and AHA against *K. pneumoniae* in M9U.

Bacterium	TA	NaF	AHA
K. pneumoniae	6.4 mmol l^{-1}	9.6 mmol l^{-1}	76.8 mmol l^{-1}

3. Results and discussion

3.1. Determination of the minimum inhibitory concentrations and anti-ureolytic effects of TA, NaF, and AHA in single-compound treatments of K. pneumoniae

The MICs of TA, NaF, and AHA against *K. pneumoniae* in M9-based urea medium (M9U) were determined using a plate reader (Table 1).

The MICs for TA and NaF were relatively high at 5–10 mmol l^{-1}. However, the MIC for AHA was almost 77 mmol l^{-1} and thus significantly greater than those for TA and NaF. This is not surprising, as TA is a known antimicrobial compound [22–24], while fluoride (F^-) inhibits several metabolic enzymes, such as urease and enolase, and is known to have toxic/inhibitory effects on bacterial cells at relatively high concentrations [25,26]. Conversely, AHA is a small synthetic drug specifically developed to inhibit urease [27, 28].

Cultures of *K. pneumoniae* in M9U were incubated in a plate reader for 24 h and the absorbances were measured at 557 nm and 630 nm. To study the anti-ureolytic effects of TA, NaF, and AHA, *K. pneumoniae* cells were cultured in the presence of TA (0.0, 0.05, 0.20, 0.40 mmol l^{-1}), NaF (0.0, 0.15, 0.30, 0.60, 1.20 mmol l^{-1}), or AHA (0.0, 0.020, 0.15, 0.60 mmol l^{-1}). In the bacterial urease activity assays, the concentrations of the compounds were chosen to be well below their MICs as the primary purpose of the study is to investigate urease inhibition in single-, dual-, and triple-compound treatments (Table 1, Supporting Information Figs. S1–S3).

Single-compound treatment of *K. pneumoniae* with TA at a concentration of 0.40 mmol l^{-1} had moderate effects on ureolytic activity and growth, delaying the onset of pH increase and growth by averages of 12.2 % and 16.2 %, respectively, relative to those of an untreated control (Supporting Information Fig. S1 and Table S1). The higher final OD630 values of the cultures treated with 0.40 mmol l^{-1} TA compared to those of the untreated cultures may be due to the precipitation of proteins and other cellular debris as the cell density increased (Supporting Information, Fig. S1). Treatment of *K. pneumoniae* with NaF at a concentration of 0.60 mmol l^{-1} delayed the onset of pH increase by 33.1 % and growth by 28 % compared to those of the untreated control cultures (Supporting Information Fig. S2 and Table S1). However, Replica 2 of the NaF-treated culture exhibited a sudden, unexplained, halt of the ureolytic pH increase after approximately 10 h, which lasted for 3 h (Supporting Information Fig. S2b). Treatment with NaF decreased the growth rate by 68 %, while the rate of ureolysis was less affected. Finally, treatment of *K. pneumoniae* with 20, 150 or 600 μmol l^{-1} AHA had very slight effects on ureolytic activity (final A557–A630) and growth relative to those of the untreated control (Supporting Information Table S1). Treatment with 20 μmol l^{-1} AHA appeared to increase the final cell density (final OD630) by 1 %, 18 %, and 23 % for the biological triplicates compared to the densities of the untreated control cultures (Supporting Information Fig. S3).

3.2. Synergistic inhibition of ureolytic activity by NaF or AHA in the presence of TA in dual-compound treatments of K. pneumoniae

To investigate the compound combination effects of TA with NaF and/or AHA, *K. pneumoniae* were cultured in the presence of 1) TA and NaF, 2) TA and AHA, or 3) TA, NaF, and AHA. The combinations always included 0.30 mmol l^{-1} TA. Combinations with NaF (0.0, 0.30, 0.60 mmol l^{-1}) or/and AHA (0, 1.2, 5, 10 μmol l^{-1}) were then assessed in 96-well plates (Table S1). At these concentrations, none of the compounds had large anti-ureolytic effects on *K. pneumoniae* in single-compound treatments (Supporting Information, Figs. S1, S2, and S3; Table S1), which allowed the identification of compound ratios that showed synergetic inhibition of bacterial ureolytic activity between TA/NaF, TA/AHA, and NaF/AHA.

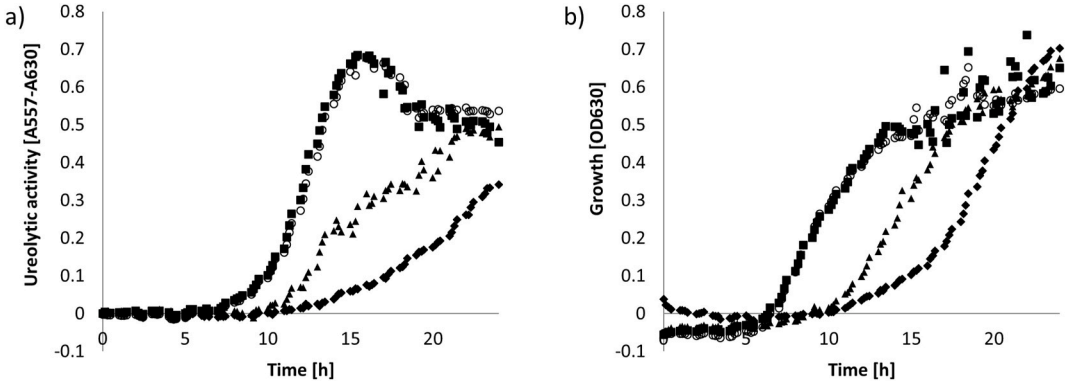

Fig. 1. Anti-ureolytic effects of NaF and AHA on *K. pneumoniae* in the presence of TA. a) Ureolytic activity (A557-A630) and **b)** growth (OD630) of untreated *K. pneumoniae* (**o**) and *K. pneumoniae* treated with 0.30 mmol l^{-1} TA and 0.60 mmol l^{-1} NaF (▲); 0.30 mmol l^{-1} TA and 10.0 μmol l^{-1} AHA (■); and 0.30 mmol l^{-1} TA, 0.60 mmol l^{-1} NaF, and 10.0 μmol l^{-1} AHA (◆). The data are from Replica 1. *K. pneumoniae* treated with 0.30 mmol l^{-1} TA and 0.60 mmol l^{-1} NaF had significantly later onset of the pH increase and growth than the untreated control. In contrast, treatment with 10.0 μmol l^{-1} AHA in the presence of 0.30 mmol l^{-1} TA did not affect the ureolytic activity or growth of *K. pneumoniae*. However, the addition of 10.0 μmol l^{-1} AHA in the presence of both 0.30 mmol l^{-1} TA and 0.60 mmol l^{-1} NaF dramatically delayed the onset of the pH increase and growth. Thus, in the presence of TA, strong synergistic effects of NaF and AHA were observed. Plots of the ureolytic activity and growth of biological replicates from Replica 2 and Replica 3 are presented in the Supporting Information (Fig. S4 a-d).

The dual-combination treatment of *K. pneumoniae* with 0.30 mmol l^{-1} TA and 0.60 mmol l^{-1} NaF resulted in, on average, a 37 % later onset of the pH increase and a 52 % increase in lag time for the biological replicates. Interestingly, the rate of pH increase was 59 % faster, while the growth rate was 46 % slower than that of the control (Fig. 1 and Supporting Information, Fig. S4 and Table S1).

The significantly later onset of the pH increase for the dual treatment with 0.30 mmol l^{-1} TA and 0.60 mmol l^{-1} NaF compared to *K. pneumoniae* with only TA (Table S1) was due to a synergistic effect between TA and NaF, as previously reported [18,20]. The dual-combination treatment of *K. pneumoniae* with 0.30 mmol l^{-1} TA and 10.0 μmol l^{-1} AHA had no effect on the onset or rate of pH increase compared to the control (Fig. 1 and Supporting Information, Fig. S4 and Table S1). A set of experiments with *K. pneumoniae* treated with a higher AHA concentration (0.30 mmol l^{-1}) and increasing concentrations of TA (0.0–0.10 mmol l^{-1}) confirmed the synergistic inhibition of ureolysis by TA and AHA in *K. pneumoniae* culture observed previously (Supporting Information, Fig. S5) [20].

3.3. Combining TA, NaF, and AHA in triple-compound treatments of K. pneumoniae resulted in strong and enhanced synergistic inhibition of the ureolytic activity

Triple-combination treatment of *K. pneumoniae* with 0.30 mmol l^{-1} TA, 0.60 mmol l^{-1} NaF, and 10.0 μmol l^{-1} AHA caused significant additional delays in the onset of pH increase and growth and additional decreases in the rates of pH increase and growth. Thus, the onset of pH increase and the end of lag phase values were, on average, 76.7 % and 80 % longer than that of the untreated control, respectively (Fig. 1 and Supporting Information, Fig. S4 and Table S1). Surprisingly, these increases were also present, with only 1.20 μmol l^{-1} AHA at 95.8 % and 124.3 %, respectively (Supporting Information, Table S1). The data suggest that in the presence of both TA and NaF, the ureolytic activity of *K. pneumoniae* is very sensitive to AHA, but the absolute amount of AHA is less important. In comparison, a previous study revealed that an 833-fold increase in the concentration of AHA (1.0 mmol l^{-1}) alone was needed to delay the onset of ureolytic activity in *K. pneumoniae* by 77 % [19]. Increasing or decreasing the concentration of NaF from 0.60 mmol l^{-1} generally led to proportional changes in the inhibition of ureolytic activity, and as an earlier study concluded, 1.0 mmol l^{-1} NaF in the absence of TA completely inhibited ureolysis of *K. pneumoniae* in pure culture [19]. The current results show an additional synergistic effect between NaF and AHA at very low concentrations of AHA when treating *K. pneumoniae*, which is very interesting considering that AHA normally has significant effects only at much higher concentrations. Notably, the recommended total oral dose of AHA should never exceed 1.5 g/d for adults [17]. Products for flushing catheters to remove incrustations are generally flushed with approximately 30 ml of fluid [29]. Flushing a catheter with 30 ml of a 10 μmol l^{-1} AHA results in 22.5 μg of AHA in total or 1/66,000 the maximum daily dose. Additionally, AHA is not expected to be absorbed from the bladder, which further reduces the risk of any side effects from low concentrations of AHA. Because bacterial ureolytic activity and growth are significantly delayed by triple-compound treatment with TA, NaF, and AHA even after 15 h, our results suggest a potential medical strategy of reducing the amount of AHA necessary for preventing the growth of ureolytic bacteria and increase of pH in the urinary tract and catheters to avoid blockage of urine excretion by incrustation.

3.4. A reduction in total bacterial ammoniacal nitrogen (TAN) production confirmed the anti-ureolytic effect of triple-combination treatment with TA, NaF, and AHA

To confirm that the pH increase quantified with the phenol red-based assay was related to ureolysis, the concentration of TAN in cultures of *K. pneumoniae* with no additives or with a triple-combination treatment of 0.30 mmol l^{-1} TA, 0.60 mmol l^{-1} NaF, and 10.0 μmol l^{-1} AHA was determined using the Kjeldahl method. M9U with an initial pH of 6.69 was inoculated with cells from an overnight culture to a starting OD630 of 0.1. After 5 h of incubation at 25 °C, the pH increased to 6.96, and the OD630 was 1.24 in the control culture. The pH of the ureolysis-inhibited culture decreased to 6.23, while the OD630 of the culture increased to 1.20. Kjeldahl measurements revealed that the uninhibited control culture contained 4747.5 ± 1070.1 mg NH_3/kg, while the triple-compound-treated *K. pneumoniae* culture contained only 853.4 ± 113.6 mg NH_3/kg. Thus, on average, the triple-combination treatment of *K. pneumoniae* with 0.30 mmol l^{-1} TA, 0.60 mmol l^{-1} NaF, and 10.0 μmol l^{-1} AHA reduced TAN production by 82 % compared to that of the untreated culture. This confirms that the delayed onset/absence of pH increase observed in the presence of TA, NaF, and AHA was caused by a reduction in NH_3 production. In contrast to the pH, the final OD630 values were nearly the same for the triple-compound-treated and control cultures after 5 h of incubation, suggesting that both cultures experienced similar growth and suggesting that the observed reduction in TAN was unlikely to be caused by a general antimicrobial effect. Furthermore, when the ureolytic activity (A557-A630) was normalized to the growth (OD630) (Fig. 1 and Supporting Information Fig. S4), the urease activity per cell density (A557-A630)/OD630 was significantly lower in the *K. pneumoniae* cultures inhibited by TA and NaF as well as TA, NaF, and AHA than in the control culture (Supporting Information, Fig. S6a). In particular, the triple-combination treatment had a strong effect, as the ureolytic activity per cell density was low and relatively constant for a long period of time. The ureolytic activity per cell density was also reduced in the dual-combination treatment with TA and NaF but increased at a constant rate during cultivation (Supporting Information, Fig. S6a). Notably, while the relationship between ureolytic activity and cell density appeared to be exponential for the control culture then it was more linear for the culture treated with TA and NaF and the culture treated with TA, NaF, and AHA (Supporting Information Fig. S6b). These results strongly suggest that the inhibitors mainly hamper the ability of cells to break down urea to ammonia and that any reduction in growth is caused indirectly by their reduced ability to increase the pH of the medium. It was recently shown that *K. pneumoniae* is able to survive at pH 7–10 while no growth is observed below pH 6 underlining its tolerance to neutral and alkaline pH as well as its susceptibility to acidic pH [30].

3.5. Synergistic inhibition of cell-free urease by NaF and AHA

To further investigate the observed synergistic inhibition of bacterial urease activity by NaF and AHA, the activity of cell-free urease in M9U was studied in the presence of NaF, AHA, or both urease inhibitors (Fig. 2). TA was not added to the enzymatic urease activity assay mixture because it precipitates the free urease enzyme immediately. Furthermore, the inhibitory effect of TA on ureolytic bacteria is believed to primarily involve an increase in membrane permeability [19,31].

In line with the bacterial assays, the presence of 10.0 μmol l^{-1} AHA did not affect the enzymatic activity of jack bean urease (JBU), while 0.60 mmol l^{-1} NaF significantly reduced the reaction rate and resulted in a lower final pH increase reflected by the lower absorbance at 557 nm after 20 h, corresponding to final pH values of 7.76 and 7.39, respectively [21]. For the cell-free urease reaction with 0.60 mmol l^{-1} NaF, the initial reaction rate decreased by 84.3 %, and the final A557 decreased by 23.3 % compared to those for untreated JBU (Fig. 2). Combining 0.60 mmol l^{-1} NaF with 10.0 μmol l^{-1} AHA in the enzymatic reaction decreased the initial reaction rate by 86.3 %, which was nearly the same as that for the mono-treatment with 0.60 mmol l^{-1} NaF, while the final absorbance decreased by 44.3 % relative to that of untreated JBU and corresponded to a pH of 7.18 (Fig. 2). Both the NaF and NaF with AHA treatments increased the time needed for ureolysis to overcome the buffer capacity of the medium from 0 to 75 min. Thus, as in the experiments with *K. pneumoniae,* the rate of pH increase was predominantly affected by the presence of relatively high amounts of NaF. Interestingly, combining NaF with a small amount of AHA appears to increase the duration of inhibition of the urease enzyme and thereby further reduce the overall pH change even though the low AHA concentration has no observable inhibitory effect when administered alone. Notably, as the pH increased during the reactions, NaF and AHA in combination appeared to be more effective than NaF alone, suggesting the presence of a pH-dependent inhibitory mechanism. However, the synergistic anti-ureolytic effect of AHA with NaF was much more pronounced when studying whole bacteria versus isolated urease enzymes.

To further compare and study the anti-ureolytic effects of NaF and AHA, the initial reaction rates of JBU treated with NaF, AHA or equimolar mixtures of NaF and AHA were determined. Titration of JBU with NaF or AHA at concentrations of 5, 20, 40, 60 and 80 μmol l^{-1} or equimolar NaF and AHA at concentrations of 20, 40, 80, 120 and 160 μmol l^{-1} showed that AHA appeared to be a more powerful inhibitor of urease than NaF, except at 5 μmol l^{-1} (Fig. S7). Surprisingly, in the enzymatic urease activity assay, the combination treatment with 50 % NaF and 50 % AHA was also less effective than AHA alone at reducing the initial rate of ureolysis. Thus, the effect of the combined inhibitors closely followed the effect of NaF alone, suggesting that fluoride binds more quickly to the active site of urease than AHA and that AHA may have difficulty binding when fluoride is present under the applied conditions. The inhibition of cell-free urease did not explain the very strong synergistic inhibition of ureolysis and growth observed in the bacterial assays, which suggested that certain conditions in the bacterial cytosol are important for this inhibition. One significant difference between the conditions in the bacteria and the cell-free urease activity assay was pH. In the cell-free assay, the initial pH was 6.8, while the pH can be significantly greater in the cytosol of *K. pneumoniae.*

3.6. Model for pH-dependent cobinding of fluoride (F^-) and AHA in the active site of urease

To the best of our knowledge, there are currently no crystal structure or modelling studies that have investigated the coinhibition of urease by mixed inhibitors, but the structure of the substrate urea bound to a fluoride-inhibited *Sporosarcina pasteurii* urease has been reported recently [32]. A structure showing the binding mode of fluoride to the active site nickel atoms of *Sporosarcina pasteurii* urease [33] and a structure showing the binding mode of AHA in the active site of *Bacillus pasteurii* urease [34] have also been published. The

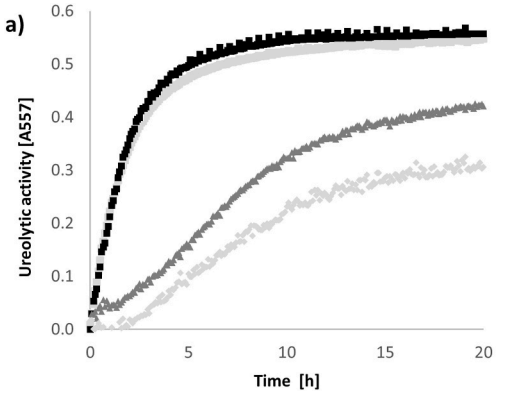

b)	Initial reaction rate [s^{-1}]	Final A557 [AU]
JBU	51.1±7.05e-6	0.549±0.05
JBU + NaF 0.60 mmol l^{-1}	8.02±1.83e-6	0.421±0.06
JBU + AHA 10.0 μmol l^{-1}	52.7±11.7e-6	0.558±0.06
JBU + NaF 0.60 mmol l^{-1} and AHA 10.0 μmol l^{-1}	6.98±0.28e-6	0.306±0.01

Fig. 2. NaF and AHA synergistically inhibited cell-free urease activity. a) Average ureolytic activity (A557) of untreated jack bean urease (JBU) (x), JBU with 0.60 mmol l^{-1} NaF (▲), 10.0 μmol l^{-1} AHA (■), or 0.60 mmol l^{-1} NaF and 10.0 μmol l^{-1} AHA (◆). The activity of JBU was not affected by 10.0 μmol l^{-1} AHA (measured initial reaction rate in the period 0–95 min), whereas 0.60 mmol l^{-1} NaF decreased the initial reaction rate significantly compared to that of the untreated JBU (measured in the period 75–133 min). The combination of 0.60 mmol l^{-1} NaF with 10.0 μmol l^{-1} AHA slightly decreased the initial reaction rate further, albeit not significantly (at 75–245 min). The maximum absorbance related to the ureolytic pH increase decreased by 23.3 % with 0.60 mmol l^{-1} NaF and 44.3 % with 0.60 mmol l^{-1} NaF and 10.0 μmol l^{-1} AHA after 20 h compared to the final A557 for the uninhibited urease reaction. **b)** The initial rates and final absorption at 557 nm obtained from the data shown in **a).**

currently accepted mechanism for fluoride inhibition of urease consists of one fluoride bridging the active site nickel atoms replacing the hydroxide bridge present in the native enzyme [33] and a second fluoride replacing a molecule of water to bind to the coordinatively unsaturated Ni1. The bridging fluoride inhibits urease in an uncompetitive manner, while the second fluoride acts as a competitive inhibitor (Fig. 3c). It was noted by the authors that the nonbridging fluoride becomes much less relevant as the pH increases. In the case of AHA and other hydroxamic acids, initial binding occurs through the carbonyl oxygen to Ni1, after which the hydroxamic acid oxygen is deprotonated, and the two nickel atoms are chelated in a bridging manner as water is lost (Fig. 3d–e). It was concluded from the crystal structure that the active inhibitor is the hydroxamate anion and not hydroxamic acid itself.

A study by Mazzei, L. et al. [32] showed that urea can bind urease in the presence of fluoride (Fig. 3b); therefore, it could be possible for the urease active site to accommodate both a fluoride ion and AHA at the same time. Based on the current observations and knowledge combined with the generally accepted mechanisms for the inhibition of urease with fluoride and AHA alone, we propose a model in which the inhibitors bind simultaneously to the active site of urease in a pH-dependent manner. Thus, we hypothesize that in the presence of both fluoride and AHA, fluoride binds quickly and causes initial inhibition of the enzyme (Fig. 3f). At acidic and neutral pH values, it is unlikely that AHA will bind to the active site as long as a fluoride is associated with Ni1. However, as the pH increases due to ureolytic activity, the binding of the second fluoride to Ni1 becomes increasingly unlikely, and simultaneously, an increasing fraction of AHA (pKa ≈8.7) is deprotonated, giving rise to a stronger attraction to the positively charged nickel atoms (Fig. 3f). Thus, the second step would only take place at any significant level at alkaline pH, whereas at low or neutral pH, urease would be inhibited by either two fluoride ions (Fig. 3c) or one AHA (Fig. 3d–e). This pH dependency explains why very little synergy was observed in the initial phase when NaF and AHA were both present with cell-free urease in M9U with a starting pH of 6.8 (Fig. 2 and Supporting Information, Fig. S7); however, as the pH increased, the activity of urease with NaF and AHA decreased more than that with only NaF (Fig. 2). The final pH during treatment with NaF and AHA was 7.39, which indicated that approximately 7.2 % of the AHA was deprotonated. The intracellular pH values of different *K. pneumoniae* strains in LB medium have been measured to be 6.8 at the start of growth but increased to 8.0–8.4 after hours of growth [35], indicating that within cells, gradually more deprotonated AHA would form as the intracellular pH increases. For example, at a pH of 7.5, approximately 9.1 % of AHA would be deprotonated compared to less than 2 % at the start of the experiment.

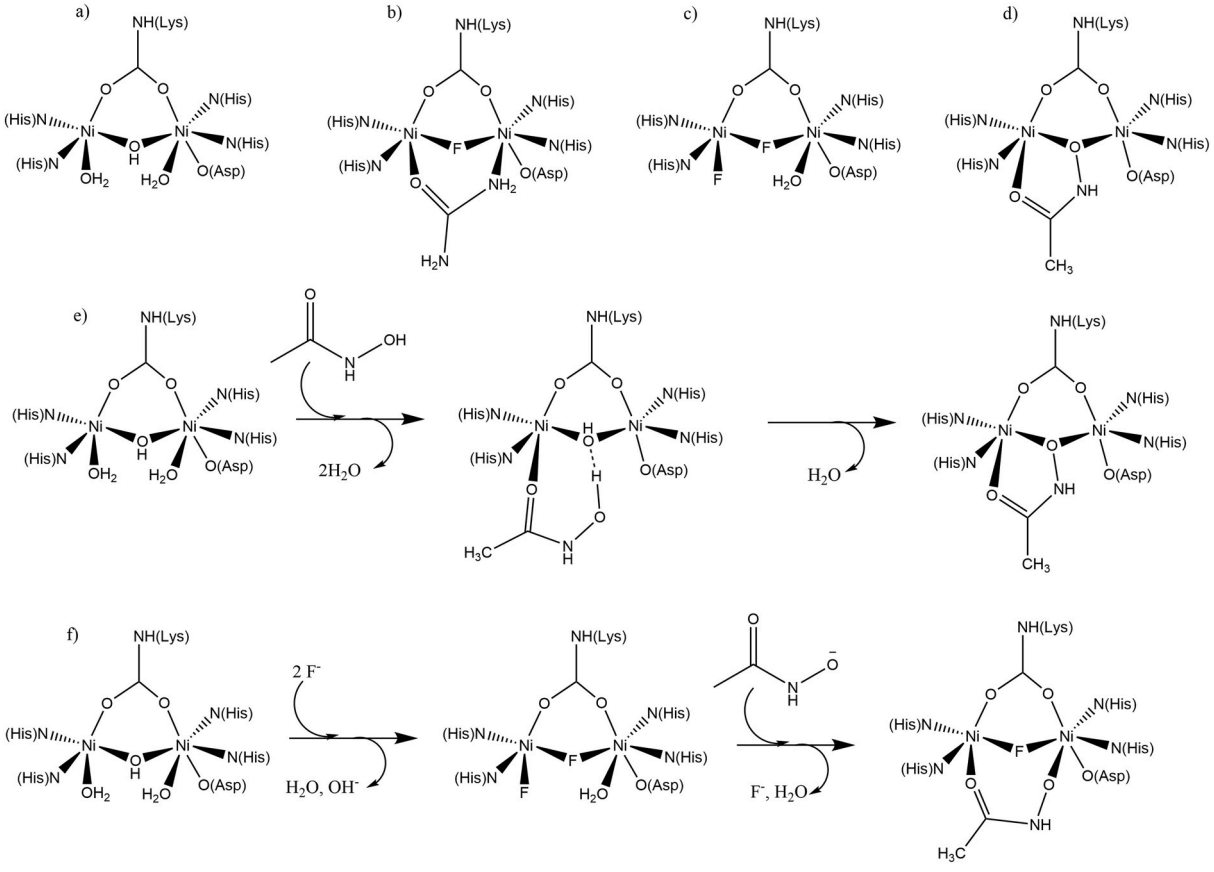

Fig. 3. Binding modes of urea, fluoride, and AHA in the active site of urease. Binding modes in the active site of a) native urease [36], b) urease cobinding urea and fluoride [32], c) fluoride-inhibited urease [33], and d) AHA-inhibited urease [34] according to crystal structures. e) Currently accepted binding mechanism of AHA in the active site of urease under acidic and neutral conditions [34]. g) Proposed mechanism and binding modes for the simultaneous binding of fluoride and deprotonated AHA in the active site of urease under alkaline conditions.

4. Conclusion

In the present study, we demonstrated that the concentration of the urease inhibitor AHA needed for the inhibition of ureolytic activity and growth of *K. pneumoniae in vitro* can be significantly reduced if AHA is coadministered with TA and NaF. Treating *K. pneumoniae* with 0.60 mmol l^{-1} AHA did not affect the growth lag phase but increased the onset of the ureolytic pH increase by 4.5 %. However, when as little as 1.20 μmol l^{-1} AHA was combined with 0.30 mmol l^{-1} TA and 0.60 mmol l^{-1} NaF, the onset of the ureolytic pH change increased by 95.8 %, and the growth lag phase increased by 124.3 %. At these concentrations, without AHA, TA and NaF increased the onset of the ureolytic pH change by 37.0 % and the growth lag phase by 52.5 %; thus, the additional inhibition was significant.

Based on previous and current results, we hypothesize that the strong synergistic effects of urease inhibition by TA, NaF, and AHA in triple-compound treatments of *K. pneumoniae* are due to increases in the overall uptake of urease inhibitors (fluoride and AHA) due to interactions of TA with the cell membrane and the subsequent cobinding of fluoride and AHA in the active site of urease at slightly alkaline pH. However, further studies are needed to reveal the exact molecular mechanism involved in the inhibition of urease when mixing fluoride and AHA inhibitors and to investigate the effects of dual- and triple-compound treatments with TA, NaF, and AHA on other ureolytic bacteria. These findings could be useful in medicine for reducing the side effects of AHA when it is used as a drug against UTIs and blocked catheters. Thus, treatment with a cocktail of TA, NaF, and AHA significantly delays ureolysis and the growth of ureolytic bacteria, providing the immune system with much longer duration of response to bacterial infection. This approach represents a novel and highly target-specific therapeutic strategy for combating ureolytic bacteria in different types of infections, as well as for preventing the formation of urinary tract stones and crystalline biofilms on catheters. None of the three compounds are antibiotics and, as such, should not promote resistance, and an anti-ureolytic cocktail may be effective at controlling carbapenem-resistant *K. pneumoniae*.

Funding

This work was supported by a grant (ManUREA Technology; File Number 34009-15-0934) from The Danish Ministry of Food, Agriculture and Fisheries and a proof-of-concept (PoC) grant from the University of Southern Denmark. The funding bodies played no role in the experimental design, data collection and analysis, preparation of the manuscript, or decision to publish.

Ethical approval

Not required.

Data availability statement

No data associated with the study has been deposited into a publicly available repository. The data supporting the findings of this study will be made available from the corresponding author (Henrik Karring) upon reasonable request.

CRediT authorship contribution statement

Simon. Svane: Writing – review & editing, Writing – original draft, Visualization, Validation, Methodology, Investigation, Formal analysis, Data curation, Conceptualization. **Mie C. Lyngsie:** Writing – review & editing, Validation, Methodology, Investigation, Formal analysis, Data curation. **Janne K. Klitgaard:** Writing – review & editing, Supervision, Investigation, Conceptualization. **Henrik. Karring:** Writing – review & editing, Writing – original draft, Supervision, Project administration, Investigation, Funding acquisition, Conceptualization.

Declaration of competing interest

The authors declare the following financial interests/personal relationships which may be considered as potential competing interests: Henrik Karring reports financial support was provided by The Danish Ministry of Food, Agriculture and Fisheries. Simon Svane reports financial support was provided by The Danish Ministry of Food, Agriculture and Fisheries. Henrik Karring has patent Mitigation of ammonia, odour and greenhouse gases issued to University of Southern Denmark. Simon Svane has patent Mitigation of ammonia, odour and greenhouse gases issued to University of Southern Denmark. If there are other authors, they declare that they have no known competing financial interests or personal relationships that could have appeared to influence the work reported in this paper.

Appendix A. Supplementary data

Supplementary data to this article can be found online at https://doi.org/10.1016/j.heliyon.2024.e31209.

References

[1] J.J. Sigurdarson, S. Svane, H. Karring, The molecular processes of urea hydrolysis in relation to ammonia emissions from agriculture, Rev. Environ. Sci. Biotechnol. 17 (2) (2018) 241–258, https://doi.org/10.1007/s11157-018-9466-1.
[2] H.L.T. Mobley, R.P. Hausinger, Microbial ureases: significance, regulation, and molecular characterization, Microbiol. Rev. 53 (1) (1989) 85–108.
[3] G. Mancuso, et al., Bacterial antibiotic resistance: the most critical pathogens, Pathogens 10 (10) (2021), https://doi.org/10.3390/pathogens10101310.
[4] R.A. Burne, Y.Y. Chen, Bacterial ureases in infectious diseases, Microb. Infect. 2 (5) (2000) 533–542, https://doi.org/10.1016/s1286-4579(00)00312-9.
[5] Y.F. Rego, et al., A review on the development of urease inhibitors as antimicrobial agents against pathogenic bacteria, J. Adv. Res. 13 (2018) 69–100, https://doi.org/10.1016/j.jare.2018.05.003.
[6] J.K. Yee, Helicobacter pylori colonization of the oral cavity: a milestone discovery, World J. Gastroenterol. 22 (2) (2016) 641–648, https://doi.org/10.3748/wjg.v22.i2.641.
[7] T.R. Brown, On the relation between variety of micro-organisms and the composition of stone in calculous pyelonephritis, J. Am. Med. Assoc. 36 (1901) 1395–1397.
[8] P. Das, et al., Formation of struvite urinary stones and approaches towards the inhibition-A review, Biomed. Pharmacother. 96 (2017) 361–370, https://doi.org/10.1016/j.biopha.2017.10.015.
[9] S. Federici, et al., Targeted suppression of human IBD-associated gut microbiota commensals by phage consortia for treatment of intestinal inflammation, Cell 185 (16) (2022) 2879–2898 e24, https://doi.org/10.1016/j.cell.2022.07.003.
[10] S. Kitamoto, et al., The intermucosal connection between the mouth and gut in commensal pathobiont-driven colitis, Cell 182 (2) (2020) 447–462 e14, https://doi.org/10.1016/j.cell.2020.05.048.
[11] M.H. Wilde, et al., Exploring relationships of catheter-associated urinary tract infection and blockage in people with long-term indwelling urinary catheters, J. Clin. Nurs. 26 (17–18) (2017) 2558–2571, https://doi.org/10.1111/jocn.13626.
[12] K.A. Getliffe, The characteristics and management of patients with recurrent blockage of long-term urinary catheters, J. Adv. Nurs. 20 (1) (1994) 140–149, https://doi.org/10.1046/j.1365-2648.1994.20010140.x.
[13] D.J. Stickler, R.C. Feneley, The encrustation and blockage of long-term indwelling bladder catheters: a way forward in prevention and control, Spinal Cord 48 (11) (2010) 784–790, https://doi.org/10.1038/sc.2010.32.
[14] A.L. Flores-Mireles, et al., Urinary tract infections: epidemiology, mechanisms of infection and treatment options, Nat. Rev. Microbiol. 13 (5) (2015) 269–284, https://doi.org/10.1038/nrmicro3432.
[15] J.A. Downey, et al., In vitro inhibition of struvite crystal growth by acetohydroxamic acid, Br. J. Urol. 70 (4) (1992) 355–359, https://doi.org/10.1111/j.1464-410x.1992.tb15787.x.
[16] X. Zhang, et al., Chelerythrine chloride: a potential rumen microbial urease inhibitor screened by targeting UreG, Int. J. Mol. Sci. 22 (15) (2021), https://doi.org/10.3390/ijms22158212.
[17] Medscape, acetohydroxamic acid (Rx) (2023) [cited 2023 01/26]; Available from: https://reference.medscape.com/drug/lithostat-acetohydroxamic-acid-342577#0.
[18] F.R. Dalby, et al., Synergistic tannic acid-fluoride inhibition of ammonia emissions and simultaneous reduction of methane and odor emissions from livestock waste, Environ. Sci. Technol. 54 (12) (2020) 7639–7650, https://doi.org/10.1021/acs.est.0c01231.
[19] S. Svane, et al., Inhibition of urease activity by different compounds provides insight into the modulation and association of bacterial nickel import and ureolysis, Sci. Rep. 10 (1) (2020) 8503, https://doi.org/10.1038/s41598-020-65107-9.
[20] H. Karring, et al., Mitigation of Ammonia, Odor and Greenhouse Gases, PCT/EP2020/052622, 2020.
[21] J.J. Sigurdarson, S. Svane, H. Karring, Development of a M9-based urea medium (M9U) for sensitive and real-time monitoring of ureolytic activity of bacteria and cell-free urease, MicrobiologyOpen (2020) e976, https://doi.org/10.1002/mbo3.976.
[22] J.A. Field, G. Lettinga, Toxicity of tannic compounds to microorganisms, in: R.W. Hemingway, P.E. Laks (Eds.), Plant Polyphenols: Synthesis, Properties, Significance, Springer US, Boston, MA, 1992, pp. 673–692.
[23] K.T. Chung, Z. Lu, M.W. Chou, Mechanism of inhibition of tannic acid and related compounds on the growth of intestinal bacteria, Food Chem. Toxicol. 36 (12) (1998) 1053–1060, https://doi.org/10.1016/s0278-6915(98)00086-6.
[24] M. Cipriano-Salazar, et al., Antibacterial activities of tannic acid against isolated ruminal bacteria from sheep, Microb. Pathog. 117 (2018) 255–258, https://doi.org/10.1016/j.micpath.2018.01.045.
[25] R.E. Marquis, Antimicrobial actions of fluoride for oral bacteria, Can. J. Microbiol. 41 (11) (1995) 955–964, https://doi.org/10.1139/m95-133.
[26] R.R. Breaker, New insight on the response of bacteria to fluoride, Caries Res. 46 (1) (2012) 78–81, https://doi.org/10.1159/000336397.
[27] S. Kumar, A.M. Kayastha, Acetohydroxamic acid-a competitive inhibitor of urease from soybean (Glycine max), Med. Chem. Res. 19 (1) (2010) S113–S114.
[28] K. Kobashi, J. Hase, K. Uehara, Specific inhibition of urease by hydroxamic acids, Biochim. Biophys. Acta 65 (2) (1962) 380–383, https://doi.org/10.1016/0006-3002(62)91067-3.
[29] BRAUN. Uro-Tainer® Twin. [cited 2023 29/08/23]; Available from: https://www.bbraun.co.uk/en/products/b50/uro-tainer-twin-subyg.html.
[30] T.S. Ajayasree, S.G. Borkar, Survival of Klebsiella pneumoniae strain borkar in pomegranate orchard soil and its tolerance to temperature and pH, Journal of Applied Biotechnology & Bioengineering 5 (4) (2018), https://doi.org/10.15406/jabb.2018.05.00153.
[31] A. Lobiuc, et al., Future antimicrobials: natural and functionalized phenolics, Molecules 28 (3) (2023) 1114, https://doi.org/10.3390/molecules28031114.
[32] L. Mazzei, et al., The structure of the elusive urease-urea complex unveils the mechanism of a paradigmatic nickel-dependent enzyme, Angew Chem. Int. Ed. Engl. 0 (0) (2019), https://doi.org/10.1002/anie.201903565.
[33] S. Benini, et al., Fluoride inhibition of Sporosarcina pasteurii urease: structure and thermodynamics, J. Biol. Inorg. Chem. 19 (8) (2014) 1243–1261, https://doi.org/10.1007/s00775-014-1182-x.
[34] S. Benini, et al., The complex of Bacillus pasteurii urease with acetohydroxamate anion from X-ray data at 1.55 A resolution, J. Biol. Inorg. Chem. 5 (1) (2000) 110–118, https://doi.org/10.1007/s007750050014.
[35] R.S. Yan, et al., Anticolonization of carbapenem-resistant Klebsiella pneumoniae by lactobacillus plantarum LP1812 through accumulated acetic acid in mice intestinal, Front. Cell. Infect. Microbiol. 11 (2021), 80425310.3389/fcimb.2021.804253.
[36] S. Benini, et al., A new proposal for urease mechanism based on the crystal structures of the native and inhibited enzyme from Bacillus pasteurii: why urea hydrolysis costs two nickels, Structure 7 (2) (1999) 205–216, https://doi.org/10.1016/s0969-2126(99)80026-4.